Med Biol Eng Comput (2012) 50:165–171
DOI 10.1007/s11517-012-0860-5

ORIGINAL ARTICLE

How the blood pool properties at onset affect the temporal behavior of simulated bruises

Barbara Stam · Martin J. C. van Gemert · Ton G. van Leeuwen · Maurice C. G. Aalders

Received: 11 August 2011 / Accepted: 5 January 2012 / Published online: 20 January 2012

Abstract The influence of initial blood pool properties on the temporal behavior of bruises is currently unknown. We addressed this important issue by utilizing three typical classes of bruises in our three-layered finite compartment model. We simulated the effects of their initial shapes, regularity of boundaries and initial blood concentration distributions (gaussian vs. homogeneous) on the hemoglobin and bilirubin areas in the dermal top layer. Age determination of bruises with gaussian hemoglobin concentration was also addressed. We found that the initial blood pool properties strongly affect bruise behavior. We determined the age of a 200-h simulated bruise with gaussian hemoglobin concentration with 3 h uncertainty. In conclusion, bruise behavior depends non-intuitively on the initial blood pool properties; hence, a model that includes shape, area and concentration distribution at onset is indispensable. Future age determination, including inhomogeneous hemoglobin distributions, will likely be based on the presented method for gaussian distributions.

Keywords Bruise · Numerical modeling · Age determination

1 Introduction

The complex pathophysiology of bruises precludes determination of the time of infliction by visual assessment of their averaged perceived color [6, 7, 18]. Color perception-based age determination is problematic because: (1) it does not account for depth of the bruise, skin pigmentation, or the observer's ability to perceive yellow [1, 4, 10, 14, 17]; and (2) neither accounts for factors that influence the rate of healing, such as depth, size, and shape [3, 11, 14, 15]. Therefore, this method is not used for legal purposes [9]. The complex pathophysiology of bruises was first acknowledged by Randeberg et al. who designed an analytical mathematical model for bruise healing based on convection and diffusion of the relevant chromophores [3, 11, 12]. We extended this model to enable simulation of 3D diffusion of hemoglobin and bilirubin in bruises of all shapes, sizes and hemoglobin spatial distributions at onset. We particularly showed how skin thickness, diffusivity of hemoglobin and bilirubin, the enzymatic conversion of hemoglobin into bilirubin, and the draining of bilirubin into the lymphatic system affect the behavior of circular symmetric bruises [15, 16]. However, how the blood pool properties at bruise onset affect bruises was not investigated. These relations cannot easily, if at all, be obtained in an in vivo setting. The aim of this paper, therefore, is to address the temporal behavior of simulated bruises in relation to varying starting blood pool properties. The criterion we use for comparison purposes is the temporal behavior of the hemoglobin and bilirubin areas in the top layer of the dermis.

We carefully selected three typical classes of bruises, summarized in Table 1, from which important differences in the temporal behavior can be expected. The first class of bruises includes four different shapes of an equal and homogeneously distributed hemoglobin area at bruise onset: (A) a circle, (B) ellipses with variable eccentricity, and (C and D) tramline bruises. A tramline bruise is a pattern often seen when an individual is struck with a stick, belt or fingers, and blood is forced to the sides of the

B. Stam (✉) · M. J. C. van Gemert · T. G. van Leeuwen · M. C. G. Aalders
Biomedical Engineering and Physics, Academic Medical Centre, P.O. Box 22660, 1100 DD Amsterdam, The Netherlands
e-mail: barbarastam@gmail.com

Table 1 Definition of the classes of bruises used for the simulations

Classes of bruises	Bruise	Shape	Ratio major/minor axes	Major axis (mm)	Hemoglobin distribution at onset (g/L)
Class 1	A	Circle	1	25	150
	B	Ellipse	4	50	150
	C	Tramline	4	35.5	150
	D	Tramline	8	50	150
Class 2	E	Clinical bruise with irregular edge	3.55	28	150
	F	Ellipse with regular edge	3.55	28	150
Class 3	G (=B)	Ellipse	4	50	150
	H	Ellipse	4	50	Gaussian, max 150
	I	Ellipse	4	75	Gaussian, max 150

impact area to form two elliptic bruises [5, 13]. The second class of bruises includes (E) a clinical bruise, described previously [16], having an irregular edge, and (F) a theoretical bruise with the same shape and area but with a regular shaped edge. The third class of bruises includes (G) a bruise with homogeneous hemoglobin concentration distribution at onset and (H and I) bruises with a gaussian hemoglobin concentration distribution, addressing that bruises may start with a spatially inhomogeneous hemoglobin concentration. Additionally, we also present a new method to determine the age of this third class of bruises.

2 Methods

2.1 Model description

Bruises were simulated by a 3D finite compartment model based on convection of hemoglobin, diffusion of hemoglobin and bilirubin, and enzymatic conversion of hemoglobin into bilirubin, described in detail elsewhere [15]. Briefly, the model consists of three layers; the subcutaneous layer, the bottom layer of the dermis, and the top layer of the dermis. We assume no blood flow to the epidermal layer because of the tight basal membrane; therefore this layer is not incorporated in the model. Both lower layers have a variable thickness depending on the location on the body, the top layer has a 400 μm fixed thickness. Here, we chose to set the thickness of the bottom layer of the dermis at 600 μm to reflect a total dermal thickness of 1,000 μm (representative for arm skin [8]). The lateral dimensions of the total grid are set at 10 cm × 10 cm, and each layer consists of 400 × 400 elements. The model assumes that the bruise starts with a pool of blood in the subcutaneous layer at $t = 0$ h, which moves into the dermis via convection and diffusion. Bilirubin is produced from hemoglobin through enzymatic conversion and both chromophores diffuse independently in the skin where bilirubin has a four times larger diffusivity than hemoglobin [15]. Finally, bilirubin is drained into the lymphatic system, a process which is described by a clearance time. The model calculates the hemoglobin and bilirubin concentrations in time steps of 0.1 h. To visualize the spatial distributions of the two chromophores in the visible top dermal layer, a false color image is constructed, with high hemoglobin concentration depicted as bright red, fading into less intense red for lower concentrations. Similarly, bilirubin was depicted in yellow. Our simulations were performed with the set of model parameters, previously used in [15], summarized in Table 2.

The chromophores within the bruise were assumed to be 'visible' at a set minimum concentration per compartment in the top layer of the dermis for both hemoglobin and bilirubin. This level was adapted from our previously chosen 1×10^{-5} mg per compartment of 0.4 mm^3 (2.5×10^{-5} mg/mm^3) [15], and set at 1×10^{-6} mg per compartment of 0.025 mm^3 (4×10^{-5} mg/mm^3), thus maintaining approximately the same concentration. The total hemoglobin and bilirubin areas of the simulated bruise were determined by adding the number of compartments in the top layer having chromophore levels equal to or above

Table 2 Parameters used for the model [15]

Parameter	Value (SI unit)
Starting concentration of hemoglobin	150 g/L
Dermal thickness bottom layer	6×10^{-4} m
Dermal thickness top layer	4×10^{-4} m
Hydraulic conductivity, K ($t = 0$ h)	1.4×10^{-1} m^4/Ns
Pressure difference, Δp ($t = 0$ h)	2.6×10^{2} N/m^2
Diffusivity hemoglobin (D_{Hb})	4.2×10^{-13} m^2/s
Diffusivity bilirubin (D_B)	1.65×10^{-12} m^2/s
Affinity (K_m)	0.24×10^{6} mol/L
Speed of conversion (V_{max})	9.4×10^{-10} mol s^{-1} mg HO^{-1}
Concentration of HO-1	5×10^{-3} g/L
Clearance time of bilirubin (τ_B)	5.4×10^{5} s

the assumed detection threshold, multiplied with the surface area of one compartment.

2.2 The three classes of bruises

Three classes of bruises (Table 1) were used to address three different issues of temporal behavior. For all these classes of bruises we use a maximum hemoglobin concentration in the starting blood pool of 150 g/L, the normal average concentration in blood vessels (Tables 1, 2).

2.2.1 *Class 1: temporal behavior of bruises with equal area but different shapes*

The total area of the blood pool at $t = 0$ was chosen to be 491 mm^2 for the four geometries, resulting in (A) a circular bruise with 25 mm diameter, (B) an elliptic bruise with a 1:4 ratio of the minor and major axes, and a 50 mm length of the major axis, (C) a tramline bruise with a 1:4 ratio of the minor and major axes, a 35.5 mm length of the major axis and a 1 mm separation between the two ellipses, and (D) a tramline bruise with a 1:8 ratio of the minor and major axes, a 50 mm length of the major axis, and a 1 mm separation between the two ellipses. We compare the hemoglobin and bilirubin areas in time for these four types of bruises.

2.2.2 *Class 2: temporal behavior of a bruise with an irregular-shaped edge*

A clinical bruise, i.e. on the lateral side of the upper arm of a 27-year-old woman, with an irregular-shaped edge was previously described [16]. The shape of this bruise approximates an ellipse with a ratio of 1:3.55 between the minor and major axes. We compare the hemoglobin and bilirubin areas in time of clinical bruise (E), and elliptic bruise (F) with regular edge and the same axes ratio of 1:3.55.

2.2.3 *Class 3: temporal behavior and age determination of bruises with an inhomogeneous, gaussian-shaped hemoglobin pool at onset*

For a bruise with an inhomogeneous hemoglobin distribution at onset we choose a Gaussian concentration distribution for the blood pool. When a vessel ruptures at bruise onset, the hemoglobin concentration surrounding this vessel will be (close to) the intra-vessel concentration, but farther away the hemoglobin concentration may be lower and an inhomogeneous subcutaneous hemoglobin concentration can occur, here assumed to form a gaussian distribution.

We defined three ellipsoid-shaped bruises. The first two with an *equal* blood pool *area*, one with a homogeneous input blood pool (G), and the other with a gaussian hemoglobin concentration distribution (H), with maximum hemoglobin concentration of 150 g/L. The third (I) has the same hemoglobin *content* as bruise G, but is gaussian distributed. This bruise therefore has a larger hemoglobin area at $t = 0$. Again, we will compare the hemoglobin and bilirubin areas in time for these three types of bruises.

2.3 Age determination

Our new method of age determination of a Gaussian hemoglobin distributed bruise utilizes not only the blood pool *area* but also the nonhomogeneous hemoglobin *concentration distribution* in the top layer of the dermis at first presentation. We used bruise H to demonstrate our method. Arbitrarily, 200 h was chosen as the moment of first presentation. Pretending this age is unknown, we used the hemoglobin and bilirubin shapes and distributions in the top dermal layer at 200 h as first measurement, neglecting data before 200 h and using all data from this moment on as 'measurements' over time.

To perform our analysis we need to estimate the input value for the subcutaneous blood pool at $t = 0$ h based on the presented distribution at $t = 200$ h. We therefore rescaled the horizontal base of the hemoglobin concentration distribution in the top dermal layer at the time of presentation (at 200 h) with factors of 1.1, 1.2, 1.3, etc., while maintaining the maximum concentration of 150 g/L. Second, with this set of estimated subcutaneous blood pools at $t = 0$ (Fig. 4a), a set of bruise simulations were performed as a function of time. Third, the 'measured' hemoglobin and bilirubin areas are time shifted to match the calculated curves in the whole set. Fourth, the square of the difference between the measured and simulated areas were determined for the whole set. Finally, the simulation which gives the lowest difference is considered to correspond to the measured bruise and the starting point of that simulation gives the predicted age [16].

Finally, to show the importance of using the hemoglobin concentration distribution in the age determination we also created a set of blood pools at onset with the same bases as the inhomogeneous set, but with a homogeneous concentration distribution. With this homogeneous set we also created a set of simulations from which the predicted age was determined.

3 Results

3.1 Class 1: temporal behavior of bruises with equal area but different shapes

Figure 1a, first column, shows the four basic shapes, A–D (Table 1). The second column 'top layer of dermis' shows, in false color, the spatial distribution of hemoglobin and bilirubin over time. At $t = 0$ h the bruise is still located

completely in the subcutaneous layer, and thus not yet visible in the top layer of the dermis. Although the starting input blood shapes had an equal area, the development and clearing of the bruises differ. The two ellipses in bruises C and D overlap after 6 and 5 h, respectively. In bruise D, at 400 h, the two ellipses are no longer visually distinguishable, whereas in bruise C this is between 500 and 600 h. The areas of the hemoglobin and bilirubin for bruises A–D over time are shown in Fig. 1b. The importance of this figure is that it shows that the combination of hemoglobin and bilirubin areas is unique at every time point; e.g. at 401.5 h, the hemoglobin areas of bruises B and C are equal, but the bilirubin areas are different.

3.2 Class 2: temporal behavior of a bruise with an irregular-shaped edge

Figures 1 (shapes E and F) and 2 show that the changes in area for the clinical bruise with irregular-shaped edges is faster than the changes in area of the ellipse with the smooth edge that approximates the clinical bruise. Also, the hemoglobin and bilirubin areas in the clinical bruise remain smaller than in the smooth edged bruise.

3.3 Class 3: temporal behavior and age determination of bruises with an inhomogeneous, gaussian-shaped hemoglobin pool at onset

3.3.1 Temporal behavior

The inhomogeneous gaussian input shapes and the homogeneous input shape of the subcutaneous hemoglobin concentration at $t = 0$ h are shown in Fig. 3a. The areas of hemoglobin and bilirubin in the dermal top layer for the three input shapes are shown in Fig. 3b. For equal area bruises G and H, the areas of gaussian bruise H become smaller than for bruise G, and bruise H resolves faster than bruise G. This can also be appreciated in Fig. 1 (shapes G and H). For the larger gaussian bruise I, the hemoglobin and bilirubin areas initially are larger than for bruise G, but

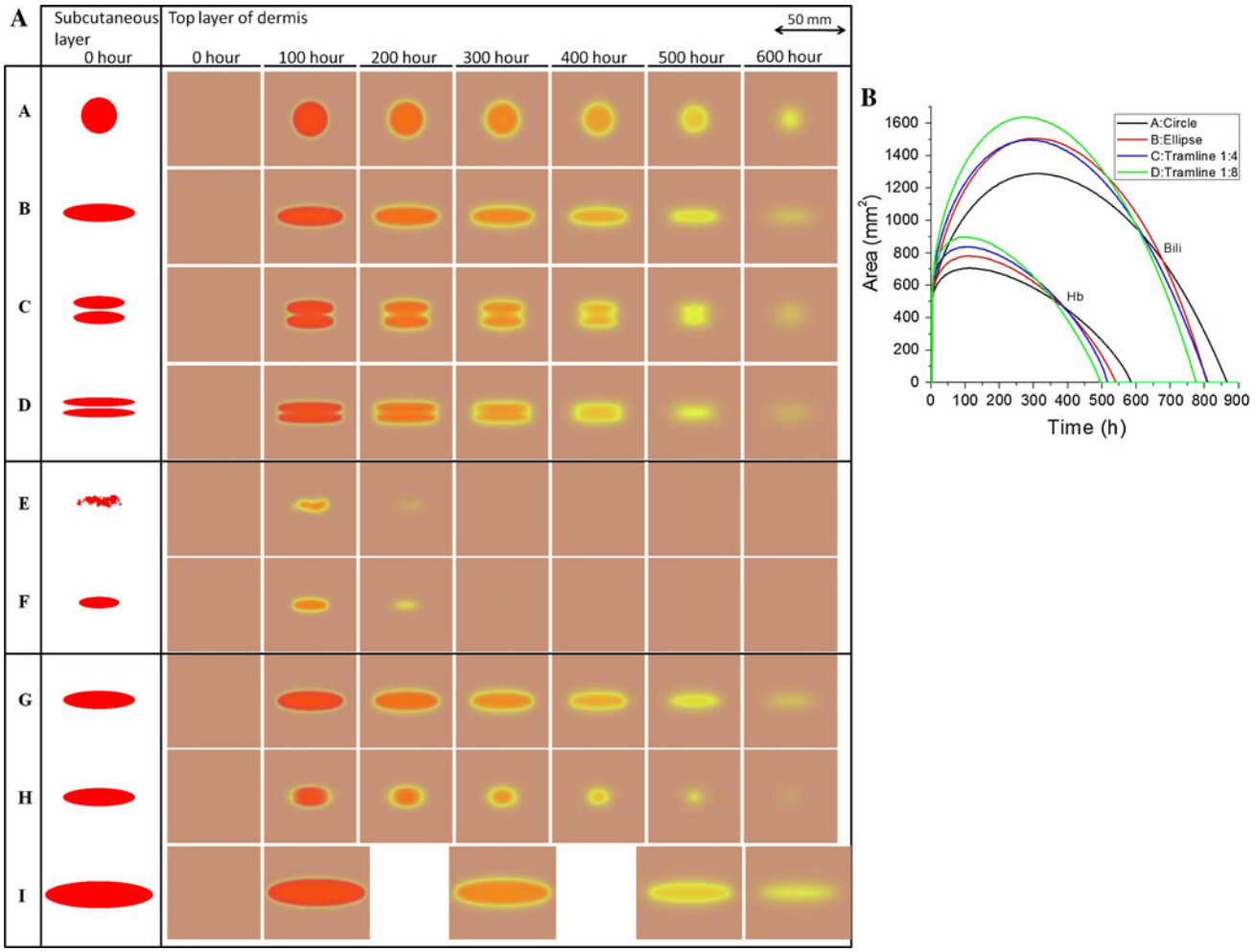

Fig. 1 **a** Spatial distributions of hemoglobin and bilirubin at different time points for all bruises *A–I*. High hemoglobin concentration depicted as intense *red*, high bilirubin concentration depicted as intense *yellow*. **b** Hemoglobin and bilirubin areas over time for bruises *A–D*

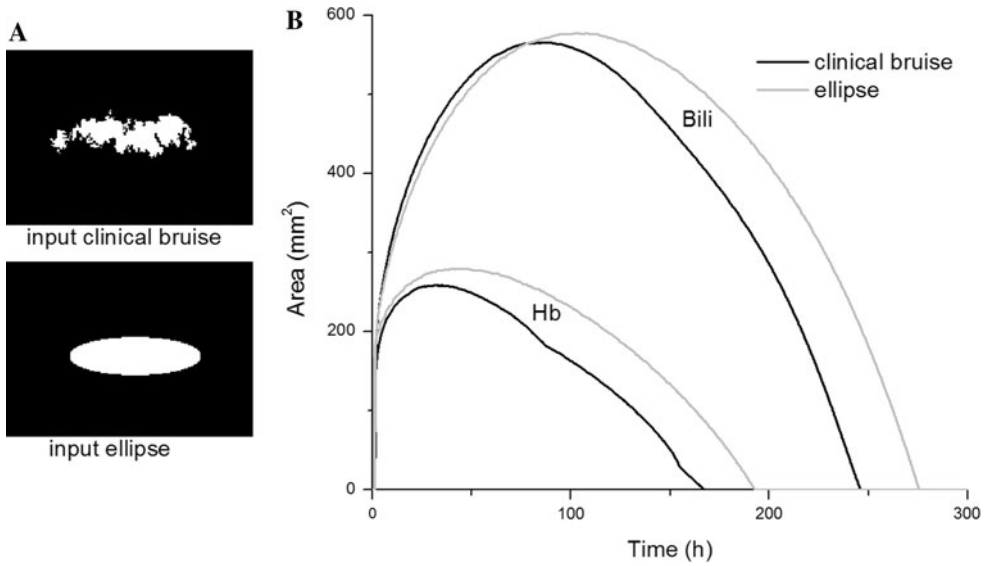

Fig. 2 **a** Hemoglobin input at $t = 0$ h in subcutaneous layer for the clinical bruise E (*top*) and its ellipse approximation F (*bottom*), both having a ratio minor/major axis of 1:3.55. **b** Hemoglobin and bilirubin areas over time for bruises E and F

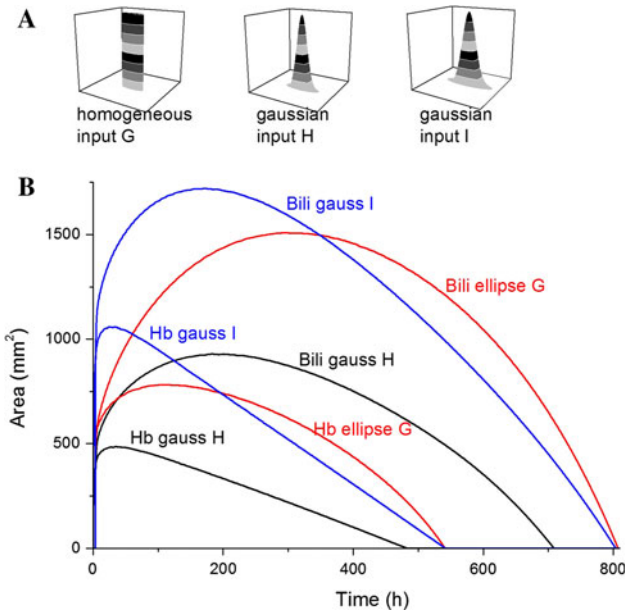

Fig. 3 **a** Homogeneous input shape *G* and nonhomogeneous gaussian input shapes *H* and *I*. *Gray levels* have no relation to concentration, but are used to better display the shape. **b** Hemoglobin and bilirubin areas over time for homogeneous input shape *G* (*red*) and gaussian input shapes *H* (*black*) and *I* (*blue*)

become smaller during the lifetime of the bruise, but bruises I and G are resolved almost simultaneously (see Fig. 1, shape I). The difference in temporal behavior between the gaussian and homogeneous input shapes is the important message here.

3.3.2 Age determination

Figure 4a shows cross-sections of the subcutaneous hemoglobin concentration at $t = 0$ h of gaussian bruise H (gray), the normalized dermal hemoglobin distribution 'measured' at 200 h (black), and, from this latter distribution, the rescaled hemoglobin distributions, used as subcutaneous inputs at $t = 0$ h for the series of simulations (shown are the 1.3, 1.6 and 1.8 rescaling factors in red, green and blue, respectively).

Figure 4b, c shows the hemoglobin and bilirubin areas, respectively, over time for the different inputs, and it can be appreciated that the simulation done with a rescaling of 1.3 times the hemoglobin distribution at 'first' presentation ($t = 200$ h) as input at $t = 0$ is optimal. This is confirmed in a series of simulations where the difference between the 'measured' and calculated areas has converged to a minimum. When we assume we measure the bruise every hour after the first presentation (at 200 h), the deviation between the new simulations and the real gaussian input is 3 h for the inhomogeneous inputs, and 32 h when a homogeneous input was assumed. In a clinical setting, measuring this frequently is probably impossible, so when we assume 2 measurements, at 200 and at 224 h, the deviation from the real age for the inhomogeneous input is 13 h, and for the homogeneous input 74 h. When we use only the measurement at 'first' presentation (200 h), the deviation from the real age for the inhomogeneous input is 52 h, and for the homogeneous input 76 h. These results show that age determination of bruises with a gaussian-distributed concentration is accurately possible if a reasonably correct concentration distribution in the blood pool at onset is taken into account.

4 Discussion

We showed that shape, size, irregularity of edges, the amount of hemoglobin and bilirubin and inhomogeneity of

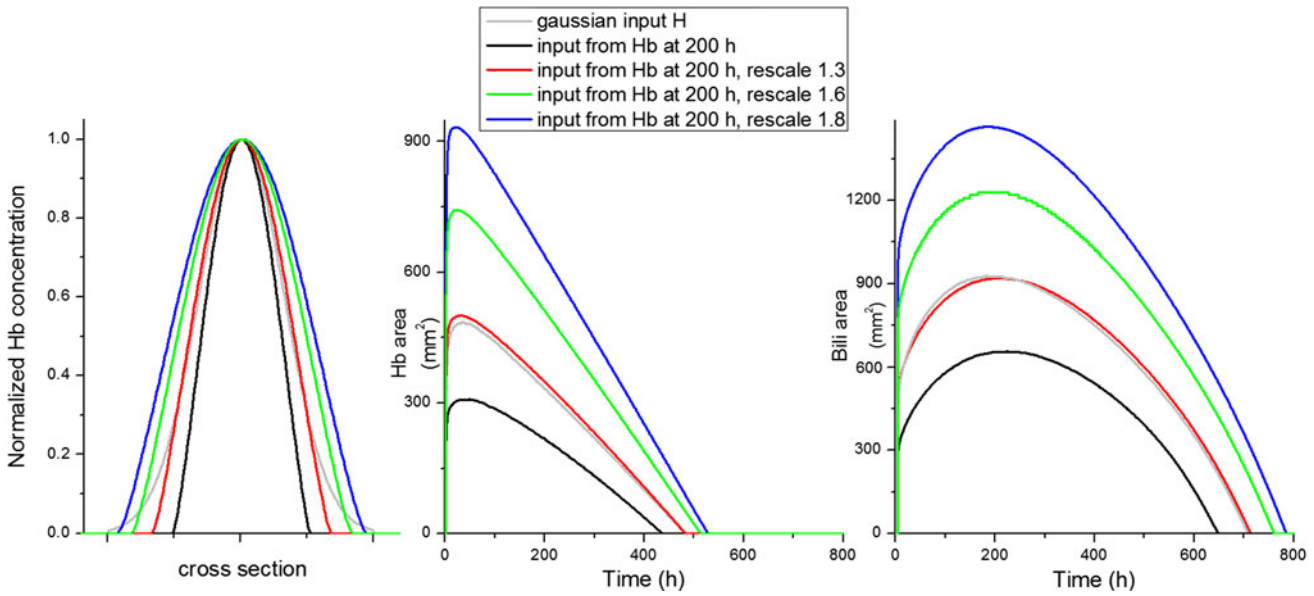

Fig. 4 **a** Cross-sections of hemoglobin distributions (normalized to 150 g/L) used as input in the subcutaneous layer for the set of simulations, with normalized gaussian bruise H (*gray*), 'measured' Hb distribution at 200 h in top layer and used as input in subcutaneous layer (*black*), and rescalings of the black input (*red*, *green*, *blue*). **b** Hemoglobin area over time for different inputs in subcutaneous layer at $t = 0$ h. **c** Bilirubin areas over time for different inputs in subcutaneous layer at $t = 0$ h

the initial hemoglobin distribution, as well as diffusivity of chromophores [15], all affect the temporal behavior of simulated bruises. An important consequence is that the observed hemoglobin and bilirubin areas in time vary non-intuitively, so a direct relation between color and age of bruises cannot be assessed, confirming clinical observations [1, 3, 17]. Thus, understanding individual bruise behavior is impossible without a sophisticated computational model, based on the actual skin pathophysiology. Trends simulated with such models give important information of bruises which cannot easily, if at all, be determined in a clinical setting.

We addressed possible consequences of a nonhomogeneous hemoglobin distribution in the initial blood pool. Such non-homogeneities can be expected when a vessel, or multiple vessels, ruptures at bruise onset and a nonhomogeneous hemoglobin distribution is formed with several areas of high and low concentrations of hemoglobin. We show differences in temporal behavior between bruises with an inhomogeneous gaussian input blood shape and a homogeneous input shape, either of equal area or equal blood volume at bruise onset, indicating that neither the initial area nor the initial blood volume can be used as a single parameter to characterize bruise development. The age determination of inhomogeneous distributed bruises shows the need for taking into account the inhomogeneity of the initial blood pool; in this way the age of the old (simulated) bruise could still be accurately determined. Previously [15, 16], we determined the age of clinical bruises from the measured hemoglobin and bilirubin areas as a function of time from the moment of first presentation, taking the chromophore concentrations as a constant over the whole area. Although we assessed the spatial distribution of hemoglobin and bilirubin in all measurements [Fig 3 of 16], this information was not incorporated in the age determination procedure. We emphasize, however, that the irregularities of the bruise edge were taken into account here.

Importantly, we hypothesize that the presented method of age determination of a gaussian input blood pool can serve as a blueprint for future age determinations. Most likely, this requires two steps: first, decomposition of the measured hemoglobin concentration spatial distribution in a set of gaussian functions; and second, construction of a set of blood pool distributions at $t = 0$ h by enlarging each diameter of the set of functions by factors such as 1.1, 1.2, etc., and simulating bruise development (inhomogeneous hemoglobin and bilirubin distributions) for each choice, until the best agreement between measured and calculated outcomes has been achieved. We are confident that this approach will increase the accuracy of bruise age determination although this obviously has still to be proven.

The visibility of the two compounds in a bruise considered here (hemoglobin and bilirubin) depends on each other; because the two compounds often are both present. The spectra of hemoglobin and bilirubin overlap and an observed color green can mistakenly be attributed to biliverdin [7], as biliverdin is rapidly converted into bilirubin [6, 15]. Although visually hemoglobin and bilirubin are

difficult to distinguish, when a bruise is measured using reflectance spectroscopy, the compounds can be identified by using a fitting algorithm on the measured spectrum [12, 16]. A fourth compound sometimes present in bruises is hemosiderin, present in the late phase of the bruise [7]. We have not considered this compound in our analysis, as the mechanism for hemosiderin production is unclear [6].

A limitation of the optics-based methodology is that edge irregularities at hemoglobin blood pool at onset cannot be identified easily in "old" bruises, and certainly not when virtually no hemoglobin is present any more because these irregularities fade away in the bilirubin spatial distribution. Thus, optics-based methodology unlikely can accurately assess the age of "old" bruises where little hemoglobin is still present.

In this paper we focused on the implications of various blood pool properties at onset. Clearly, this is not the only factor influencing the temporal behavior of bruises. Factors such as tissue edema or gravity may also play a role, but as discussed previously [15], these factors are not (yet) included in the model at this stage. Also, the extent of the trauma to the skin may play a role, as damaged structures cause increased diffusivity of chromophores. All these factors need to be incorporated in the model and considered in future research to estimate their influence on the temporal behavior of bruises.

Multiple (confluent) bruises caused by an additional abuse before the first bruise has healed were not simulated, although the model does allow the addition of a second blood pool [15]. We felt there is insufficient pathophysiology knowledge available here. For example, how can we get knowledge on the hemoglobin concentration of the second bruise when formed on top of an existing bruise with already decreasing hemoglobin content? Also, what are the hemoglobin and bilirubin diffusivities and the Michaelis–Menten kinetics parameters if such abuses occur frequently and wound healing may have adapted to this situation, e.g. by a faster healing sequence as is shown to occur in experimental animal wounds [2]. Nevertheless, when more information becomes available, confluent bruises can easily be simulated by our code, which hopefully results in identifying criteria for recognition of multiple abuse events and the time difference between such events.

In conclusion, bruise behavior depends non-intuitively on a large number of bruise and skin parameters. Hence, it would be expected that color behavior would not reveal the age of bruises with any accuracy. Understanding bruise behavior requires a sophisticated computational model of bruise pathophysiology that accounts for all these variables. Future age determination, including inhomogeneous hemoglobin distributions, will likely be based on the presented method for gaussian distributions.

Acknowledgments Funding was provided by NWO/STW VIDI Grant Nr. AGT 7547.

References

1. Bohnert M, Baumgartner R, Pollak S (2000) Spectrophotometric evaluation of the colour of intra- and subcutaneous bruises. Int J Legal Med 113(6):343–348
2. Hamdy MK, Kunkle LE, Rheins MS, Deatherage FE (1957) Bruised tissue III: some factors affecting experimental bruises. J Anim Sci 16:496–501
3. Hughes VK, Langlois NEI (2010) Use of reflectance spectrophotometry and colorimetry in a general linear model for the determination of the age of bruises. Forensic Sci Med Pathol 6(4):275–281
4. Hughes VK, Ellis PS, Langlois NEI (2004) The perception of yellow in bruises. J Clin Forensic Med 11(5):257–259
5. Kaczor KMS, Pierce MC, Makoroff K, Corey TS (2006) Bruising and physical child abuse. Clin Pediatr Emerg Med 7(3):153–161
6. Langlois NEI (2007) The science behind the quest to determine the age of bruises—a review of the English literature. Forensic Sci Med Pathol 3(4):241–251
7. Langlois NE, Gresham GA (1991) The ageing of bruises: a review and study of the colour changes with time. Forensic Sci Int 50(2):227–238
8. Lee Y, Hwang K (2002) Skin thickness of Korean adults. Surg Radiol Anat 24(3–4):183–189
9. Maguire S, Mann MK, Sibert J, Kemp A (2005) Can you age bruises accurately in children? A systematic review. Arch Dis Child 90(2):187–189
10. Munag LA, Leonard PA, Mok JY (2002) Lack of agreement on colour description between clinicians examining childhood bruising. J Clin Forensic Med 9(4):171–174
11. Randeberg LL, Haugen OA, Haaverstad R, Svaasand LO (2006) A novel approach to age determination of traumatic injuries by reflectance spectroscopy. Lasers Surg Med 38(4):277–289
12. Randeberg LL, Larsen EL, Svaasand LO (2009) Characterization of vascular structures and skin bruises using hyperspectral imaging, image analysis and diffusion theory. J Biophotonics 3(1–2):53–65
13. Reijnders UJ, van Baasbank MC, van der Wal G (2005) Diagnosis and interpretation of injuries: a study of Dutch general practitioners. J Clin Forensic Med 12(6):291–295
14. Schwartz AJ, Ricci LR (1996) How accurately can bruises be aged in abused children? Literature review and synthesis. Pediatrics 97(2):254–257
15. Stam B, van Gemert MJC, van Leeuwen TG, Aalders MCG (2010) 3D finite compartment modeling of formation and healing of bruises may identify methods for age determination of bruises. Med Biol Eng Comput 48(9):911–921
16. Stam B, van Gemert MJC, van Leeuwen TG, Teeuw AH, van der Wal AC, Aalders MCG (2011) Can color inhomogeneity of bruises be used to establish their age? J Biophotonics 4(10):759–767
17. Stephenson T (1997) Ageing of bruising in children. J R Soc Med 90(6):312–314
18. Wilson EF (1977) Estimation of the age of cutaneous contusions in child abuse. Pediatrics 60(5):750–752